THE UNIVERSITY of EDINBURGH

Edinburgh Research Explorer

Hydrogen storage in saline aquifers

OPEN ACCESS

Hydrogen Storage in Saline Aquifers: The Role of Cushion Gas for Injection and Production

[1]Heinemann, N., [1]Scafidi, J., [2]Pickup, G., [1]Thaysen, E.M., [1]Hassanpouryouzband, A., [1]Wilkinson, M., [3]Satterley, A.K., [3]Booth, M.G., [1]Edlmann, K., [1]Haszeldine, R.S.

[1]School of Geosciences, University of Edinburgh, Edinburgh (UK)

[2]Institute of GeoEnergy Engineering, Heriot-Watt University, Edinburgh (UK)

[3]CGG Services (UK), Crompton Way, Crawley, RH10 9QN (UK)
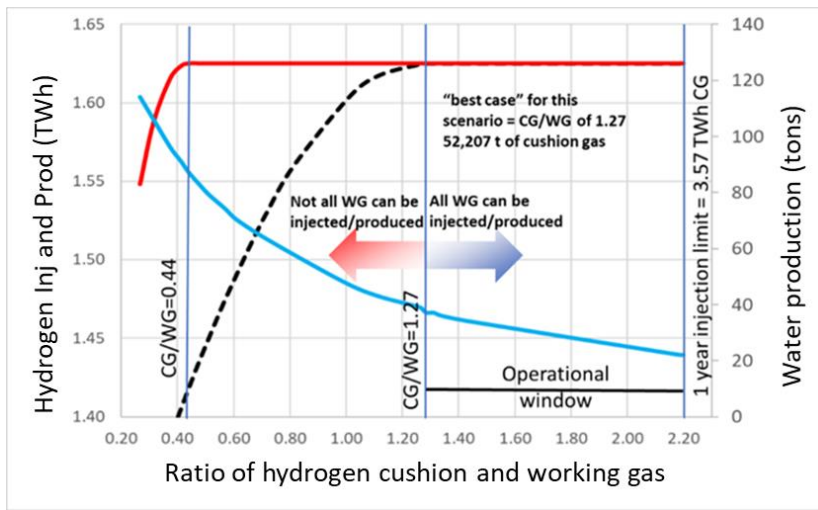
Abstract

Hydrogen stored on a large scale in porous rocks helps alleviate the main drawbacks of intermittent renewable energy generation and will play a significant role as a fuel substitute to limit global warming. This study discusses the injection, storage and production of hydrogen in an open saline aquifer anticline using industry standard reservoir engineering software, and investigates the role of cushion gas, one of the main cost uncertainties of hydrogen storage in porous media.

The results show that one well can inject and reproduce enough hydrogen in a saline aquifer anticline to cover 25% of the annual hydrogen energy required to decarbonise the domestic heating of East Anglia (UK). Cushion gas plays an important role and its injection in saline aquifers is dominated by brine displacement and accompanied by high pressures. The required ratio of cushion gas to working gas depends strongly on geological parameters including reservoir depth, the shape of the trap, and reservoir permeability, which are investigated in this study. Generally, deeper reservoirs with high permeability are favoured. The study shows that the volume of cushion gas directly determines the working gas injection and production performance. It is concluded that a thorough investigation into the cushion gas requirement, taking into account cushion gas costs as well as the cost-benefit of cushion gas in place, should be an integral part of a hydrogen storage development plan in saline aquifers.

Keywords

- Hydrogen subsurface storage
- Saline aquifers
- Low-carbon energy storage
- Cushion gas requirement

Graphical abstract

Introduction

The IPCC's 1.5 °C Report states that hydrogen must play a significant role as a fuel substitute to limit global warming and that it will lead to emission reductions in energy-intensive industries (IPCC, 2018). Stored hydrogen energy can help alleviate the main drawbacks of renewable energy generation, notably their intermittency and their seasonal and geographical constraints. The generation of renewable energy is strongly dependent on seasonally fluctuating atmospheric events such as sunlight and wind (Engeland et al., 2017), which results in renewable energy often either exceeding energy demand or leading to energy deficits. Excess renewable energy can be converted to hydrogen through electrolysis (''green hydrogen'') and stored to be used during periods of high-energy demand and hence improve energy security and reduce energy curtailment. Alternatively, hydrogen can be reformed from methane and in combination with Carbon Capture and Storage (CCS) acts as a low-carbon energy source.

Surface hydrogen storage facilities, such as pipelines or tanks have limited storage and discharge capacity (MWh; hours-days). By contrast, to supply energy in the GWh/TWh-range over weeks to months, subsurface storage of hydrogen in salt caverns, depleted hydrocarbon reservoirs and saline aquifers is needed (Matos et al., 2021, Wallace et al., 2021, Heinemann et al., 2018). Salt caverns have been used for hydrogen storage at Teeside (UK) and at the US Gulf Coast (European Commission, 2015; Panfilov, 2016). Although salt cavern storage is ideal for short- to medium-term energy demand fluctuations and allows multiple injection and reproduction cycles per year, salt cavern storage can only be implemented in regions characterised by the presence of evaporitic rock formations with suitable thickness and extent. For the decarbonisation of entire energy sectors and regions, large-scale storage in porous media, such as depleted gas fields and saline aquifers, is considered more promising (Heinemann et al., 2021).

Working Gas (WG) is the gas volume that that can be injected, stored and withdrawn during the normal commercial operation in a gas storage facility. One of the uncertainties of hydrogen storage in porous media is the amount of Cushion Gas (CG). CG is required to maintain operational pressure and maintain desired production levels. In storage scenarios with flowing water present, such as saline aquifers, the CG will also prevent excessive water inflow during production. CG is an upfront investment and an accurate determination of the CG volume required is crucial for a reliable estimation of the total storage cost. Previous literature on natural gas storage sites suggests a higher CG demand for storage in saline aquifers compared to depleted gas fields (Le Fevre, 2013). However, to date there is no study on the CG requirement for hydrogen storage in saline aquifers. Therefore, this study aims to comprehensively address the CG volume requirement for saline aquifers.

For this study, the commercial reservoir simulator GEM (CMG, 2019) was used to model the CG demand for hydrogen storage in an open, unconfined, saline aquifer to decarbonise a quarter of the domestic heating of East Anglia (UK). The study aims to answer three principal questions regarding the storage of hydrogen in open saline aquifers: A) What is the ratio of CG to WG (CG/WG) for both the WG injection and production process, and what are the scientific processes determining this ratio? B) How will fundamental geological storage parameters, in this case the reservoir permeability, the shape of the storage anticline and the storage depth, change the CG/WG ratio? C) How will the ratio change with an increasing number of storage cycles.

Porous media storage options

Gas storage in porous media has been conducted for natural gas and town gas for decades. Currently, there are 85 aquifer sites and 476 depleted oil and gas fields sites, respectively (Tarkowsky 2019). In this study, depleted oil fields are not considered due to the additional complexity of dealing with three phases (oil, gas, water). The characteristics of an open saline aquifer for hydrogen storage are best described when compared with fully confined depleted gas fields. These are endmembers and many gas fields that are not fully confined can be better described as gas filled trap structures that are part of a saline aquifer. For these fields, characteristics from both endmembers are relevant depending on the geology and hydrology of the individual fields.

The reservoir operation

Open saline aquifers are usually hydrostatically pressured. When injecting in such a reservoir, the in-situ brine is displaced leading to an increase in pressure, which can restrict injection rates. As saline aquifers are brine saturated, two-phase flow of hydrogen and brine will be the main process. Fully confined depleted gas fields are often under-pressured after years of production, and due to the lack of flow boundaries this pressure state will not equilibrate significantly during the time of interest. Depleted gas fields have a lower saturation of flowing water and contain residual gas. Therefore, injecting hydrogen will trigger the compression of the in-situ gas as well as gas mixing, which leads to the contamination of hydrogen (Tarkowsky 2019).

Risks associated with site selection

Open saline aquifers are often poorly characterised compared to depleted gas fields because their exploration has little commercial value to the oil and gas industry. Most reservoir and caprock information comes from dry exploration wells and the nature of potential trap structures is retrieved from seismic data, where available. The well density in saline aquifers is generally low and hence the risk of leakage via abandoned wells, considered as a major threat to containment, is low (Alcalde et al., 2019). Depleted gas fields on the other hand are well investigated due to decades of gas production, or even gas storage activities. The presence of multiple wells is regarded as a concern and must be assessed for the level of containment risk.

Size and location

Saline aquifers are present in most sedimentary basins worldwide, however not all are fully open. Their size can be very large and individual anticlines, which could be targeted for storage, can also be significant in size, such as the Bunter Sandstone dome structures (Williams et al., 2013). Examples of open aquifers are the Forties Formation or the Bunter Sandstone Formation located in the North Sea.

The occurrence of depleted gas fields is restricted to gas play provinces with additional faulting that provides the compartmentalisation of the fields. A known example for such a province is the Southern North Sea Permian Basin. Recent publications provide static capacity data defining how much space there is in depleted gas fields in the North Sea and show that the static capacities are large with some fields offering enough to fuel energy sectors of small countries (Scafidi et al., 2021; Mouli-Castillo et al., 2021). Nevertheless, the capacity of all porous media gas storage sites is best

defined by the volume of gas that can be injected and produced over the desired timescale. Future research has to reveal how these hydrogen storage sites can be managed, and how the storage process can be optimised.

Infrastructure and investment costs

Hydrogen storage sites in saline aquifers will most likely not have any infrastructure in place and new infrastructure investment is required. However, infrastructure costs could be reduced by choosing aquifer sites close to, e.g., already existing but redundant pipelines. Depleted gas fields on the other hand are connected to an entire industrial network combining pipelines, wells and production platforms. This has been regarded as a major factor to reduce upfront investment costs in future CO_2 storage projects (Alcalde et al., 2019). This could also be the case in hydrogen storage if the legacy-infrastructure is certified as hydrogen compatible.

Microbial activity

The injection of hydrogen into the underground may stimulate microbial activity, given that chemical energy to support life is present and that the environmental conditions are favourable for microbial growth (Thaysen et al., 2021). This may lead to a range of adverse effects such as hydrogen loss, hydrogen contamination with other gases, well corrosion and clogging of the pore space and well structures (Gregory et al., 2019). Microbial growth may be supported for a long time in unconfined saline aquifers that may see nutrient replenishment by flowing groundwater. Depleted gas fields, on the other hand, hold residual hydrocarbons which sustain the microbial community (Basso et al., 2009), but the inflow of other essential nutrients is limited due to the confined nature of the fields and insignificant surface recharge to deep subsurface environments (Wilhelms et al., 2000). The microbial activity at any site is site-specific, depending on the microbial community that is present, the nutrient supply and the temperature, pressure, pH and salinity conditions.

Methodology

Hydrogen demand scenario

Mouli-Castillo et al. (2021) presented a source to sink analysis that matches geological storage capacity with the hydrogen demand of regions in the UK. Hydrogen that could balance the annual cyclicity in energy demand, would be stored in porous media offshore and transported to the consumer via offshore pipelines, gas terminals and the onshore gas distribution network. The total calculated hydrogen energy demand is estimated to be ~77.9 TWh, of which 6.5 TWh would be transported to the area of East Anglia, located in the east of the UK. This study aims to simulate the injection, storage and reproduction of 25 % of the annual hydrogen energy demand of East Anglia, 1.625 TWh, using one well in a brine filled saline aquifer anticline storage site. This amount of hydrogen is not chosen randomly but fits the modelled constraints and additionally provides a scenario to help the reader to put the research findings into a real-world perspective. For all energy conversions within this study, a higher heating value for hydrogen of 39.4 kWh/kg is used.

Reservoir model

For this study, a 3D anticline reservoir model with a thickness of 100 m was created using Petrel (Schlumberger). The top of the reservoir is at 1500 m and the height difference between crest and base is 250 m for the base case, which corresponds to a 10° dip angle in the limbs of the structure. The water depth is 100 m, the reservoir model has a radius of 2000 m and the top and the bottom surfaces are no-flow boundaries. The reservoir model has 121,680 cells (50 x 50 m in the horizontal and 5 m in vertical direction). The centre part of the model includes a grid refinement where each cell is divided into eight cells with the dimensions of 25 x 25 m horizontal and 2.5 m vertical. Rock properties are homogenous with a horizontal permeability of 200 mD and a vertical permeability of 50 mD. The porosity is 20 %. Pressures, fracture pressure, temperature and rock compressibility are taken from Bentham (2006) and Gammer et al. (2011), collated in Williams et al. (2013) for their investigation of CO_2 storage in the Bunter Sandstone Formation in the North Sea (Table 1). The maximum allowable pressure is 90 % of the calculated fracture pressure. The salinity is set to 3.13 gmol NaCl / L, an average of North Sea and East Irish Sea pore water salinities compiled by Gluyas & Hichens (2003) and the Oil and Gas Authority website (https://www.ogauthority.co.uk/data-centre/). This study uses 2-phase flow data from Yekta et al. (2018) who measured hydrogen flow in water saturated sandstones under subsurface pressure and temperature conditions. Capillary pressure is ignored in this study.
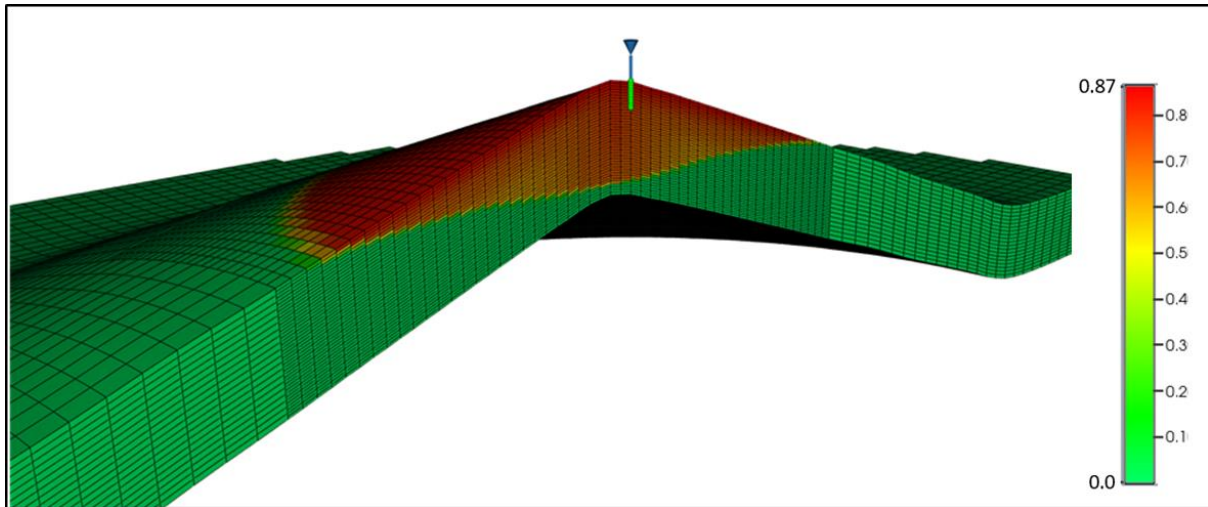
Figure 1: Simulation setup showing the reservoir model using GEM (CMG, 2019). The injection and production well is centred at the crest of the anticline structure, with the 25 m perforation in green circles. The colours show the hydrogen saturation in the brine filled reservoir model (see key for gas saturation values).

Potential storage sites, which are a part of a larger aquifer, often have an uncertain pressure dissipation during injection and production due to a lack of data. For this project, a Fetkovitch analytical aquifer is used to model pressure dissipation of a reservoir in a large-scale aquifer system (Fetkovitch, 1971). The aquifer has the same properties as the reservoir model and the radius of the entire modelled aquifer is 100 km.

Additional models were constructed with shallower limb angles of 5° and 7.5° tilt for these models the grid had to be extended to guarantee that the base of these low-angle anticlines consistently reached a depth of 1750 m, similar to the other reservoir models. For consistency, the aquifer model was adjusted accordingly.

Table 1: Reservoir pressure and temperature conditions (taken from Williams et al. (2013)

Hydrostatic gradient (MPa/km)	10.07
Lithostatic gradient (MPa/km)	22.7
Fracture pressure (MPa/km)	18
Temperature gradient (°C/km)	3.65
Surface Temperature (°C)	4

The compositional reservoir simulator GEM (CMG, 2019) was used for this study (Figure 1). During injection and production, the mobility contrast between brine and hydrogen gives rise to a high tendency for unstable, inefficient displacement, including gravity overriding and viscous fingering (Paterson, 1983; Feldmann et al., 2015). However, the homogenous field-size scenario is too coarse to take account of such small–scale phenomena. The dissolution of hydrogen in brine is neglected because it is very low, roughly one order of magnitude less compared to the dissolution of CO_2 in brine (Carden and Paterson, 1979). Diffusion of hydrogen into brine is also not taken into account because earlier work has identified it to be very low (Amid et al., 2016).

Reservoir simulators designed for the petroleum industry often use cubic Equations of State. More sophisticated Equations of State for hydrogen, such as the Leachman et al. (2009) or GERG-2008 (Kunz & Wagner, 2012), produce slightly more accurate results for subsurface conditions but have not been implemented in standard reservoir simulators. This study uses the Soave-Redlich-Kwong Equation of State to model hydrogen properties because it matches the Leachman et al. (2009) density data sufficiently well for the required pressure and temperature conditions.

Hydrogen has a low viscosity, varying roughly between 0.009 to 0.011 cP for all realistic porous media storage conditions. The common method to calculate gas viscosities implemented in commercial reservoir simulators was developed and published by Jossi et al. (1962) and further developed by Lohrenz et al. (1964) for fluid mixtures. However, Stiel and Thodos (1961) write in their early paper that the viscosity equations are applicable to all nonpolar gases, with the exceptions of hydrogen and helium, and presented alternative equations for these two fluids. Therefore, the hydrogen viscosity calculation used in this study under-predicts the more accurate Leachman et al. (2008) viscosities by more than 10 %. However, although 10 % may sound like a significant deviation, it should be considered that the absolute viscosity numbers are very low and hence 10 % of 0.009 cP is a very small inaccuracy in absolute values.

This study assumes one hydrogen injection and production well positioned at the crest of the structure. GEM (CMG, 2019) calculates the reservoir flow rate using a generalized Peaceman well model (Peaceman, 1983, 1987). The pressure loss between the reservoir and the surface is calculated using a modification of the Aziz and Govier (1972) mechanistic wellbore model. The perforation of the vertical well comprises the upper 25 m of the reservoir with a well diameter of 0.1143 m (4.5 inches). A skin factor of zero is applied which implies no alteration to the formation around the well bore for this well model.

Scenario schedule
For the hydrogen injection process, the bottom-hole pressure (BHP) of the well must not exceed the maximum allowable pressure. Once the BHP reaches this limit, the injection rate has to be reduced in order to continue injecting. An additional constraint is added to prevent water breakthrough at the production well. If the cell underneath the perforation reaches a gas saturation of 70 % or lower, the well shuts in and production stops. For the production process, the minimum well-head pressure (WHP) is set to 5 MPa, taken from the current requirements for natural gas transmission in the UK (Amid et al., 2016; Dodds et al., 2013). If the hydrogen pressure at the well-head drops below 5 MPa, no gas can flow and as a consequence, the production rate has to be lowered to allow the pressure in the well to build up and to the well to keep producing.
Cushion Gas is injected during the first year of operation. The amount of CG depends on the time of injection, hence on the scenario, and the injection process is constrained by the maximum allowed pressure. The maximum duration of CG injection is one year. After the first year of operation, the second year starts with a rest-phase of 5 months for the reservoir to equilibrate. Subsequently, the injection of the WG occurs during the summer months June – August, followed by a three month rest-phase. WG production commences at the beginning of December and continues for 91 days during winter. After production ceases, the model is terminated. For the WG, the targeted injection and production rate for the designed scenario is 1.625 TWh, 41,244 tons, of hydrogen for a three month (91 days) injection and production cycle. The targeted injection and production rate is 453

tons per day; a successful run injects and produces this amount per day for 91 days. The injection and production cannot exceed this day rate. The aim of this study is to present the CG/WG ratios as accurately as possible, and multiple scenarios were run so the ratios have an accuracy of CG/WG < +/- 0.03 at ratios of interest.

In addition to the base case, sensitivity studies on three basic geological parameters are conducted to highlight their impact on the CG requirement in hydrogen storage. These parameters and the investigated ranges are, firstly, depth (1000 m – 2000 m depth range), secondly, the openness of the anticline measured as the degree of the limb angle from horizontal (5° – 15°) and thirdly the reservoir permeability (100 mD / 25 mD – 400 mD / 100 mD for horizontal permeability / vertical permeability, respectively, table 2).

Finally, the impact of multiple hydrogen storage cycles is simulated by adding two storage cycles to the base case scenario. In order to keep the amount of CG constant, the production cycles are limited to only reproduce the volume of WG that is injected during the injection phase. This procedure guarantees that the second and the third WG cycle are still based on the initial amount of CG. For this scenario, only the injection performance is plotted because the injection is the controlling action, and the production always has to be reduced to match the injection.

Table 2: Scenario parameters for the base case and the sensitivity tests.

Parameter under investigation	Base case	Additional scenario ranges
Depth	1500 m	1000 – 2000 m
Anticline limb angle	10^0	$5\text{-}15^0$
Reservoir permeability (vertical)	50	25 – 100 mD
Reservoir permeability (horizontal)	200	100-400 mD

Results

Hydrogen injection and production

Figure 2 shows the injection and production rate as well as the BHP and WHP from a typical simulation run. During the CG injection stage, the injection rate increases rapidly and then stabilises, controlled by injection at the maximum allowable BHP. The density of the hydrogen in the reservoir is relatively high and constant (~15.3 kg/m^3) during this stage and no further gas compression is possible. Hence, the dominant process occurring during the CG injection is the displacement of brine by the injected hydrogen.

Once the CG injection ceases, the reservoir pressure equilibrates and the density of the hydrogen decreases. This expansion of the hydrogen plume during the rest-phase leads to further brine displacement. When injection of the WG starts, the BHP and the hydrogen density increases again. There is a distinct difference between the constant but high BHP and hydrogen density with a relatively low injection rate during the CG injection and the increasing BHP and hydrogen density in combination with a much higher injection rate during the WG injection. In the presented scenario, the WG injection is predominantly facilitated by CG compression. Once the BHP reaches the maximum allowed BHP, the injection rate is reduced.
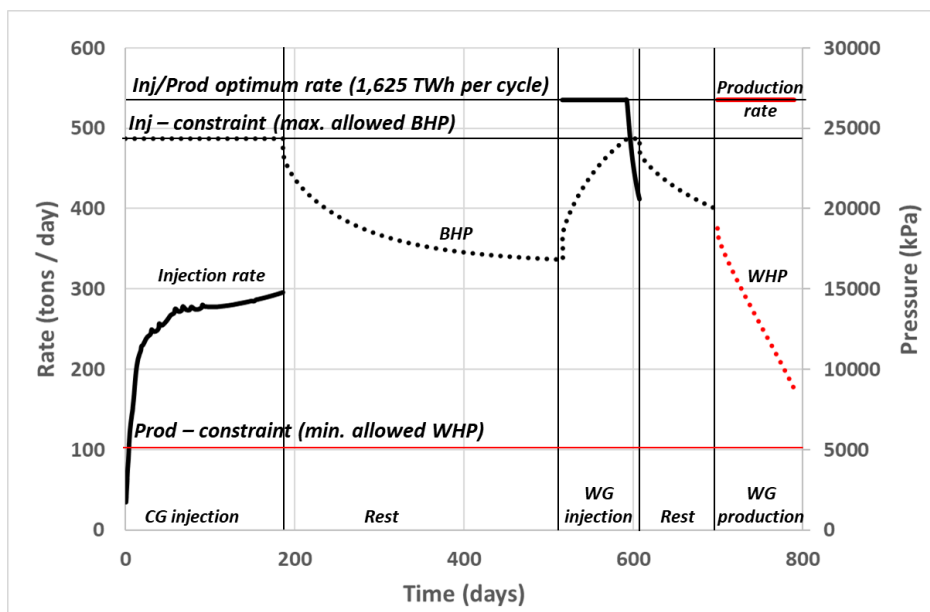

Figure 2: The development of the injection and production rates (solid lines), and the BHP and WHP (dotted lines), during simulation run used for this study. Highlighted are the maximum allowed injection and production rates (Inj/Prod optimum rate), the maximum allowed BHP (Inj-constraint) and the minimum allowed WHP (Prod-constraint).

The near well bore pressure of two WG injection scenarios is shown in Figure 3, one with a small and the other one with high volumes of CG (resulting in brine displacement dominated or compression dominated storage, respectively). The pressure at the start of the injection is lower with a small volume of CG, due to a longer pressure equilibration duration and a shorter hydrogen column height, and then increases rapidly until it reaches the maximum allowed pressure where the injection rate must be reduced to avoid compromising the reservoir. The rapid pressure increase

corresponds to an equally rapid increase in hydrogen density due to the necessary displacement of brine to make space for the injected hydrogen. The high CG volume scenario has a higher starting pressure, due to less time for pressure equilibrium and a larger hydrogen column height. Once injection commences, the pressure increases slower relative to the low CG example due to the greater volume of compressible CG. After 91 days, all the WG is injected without reaching the maximum allowed BHP.
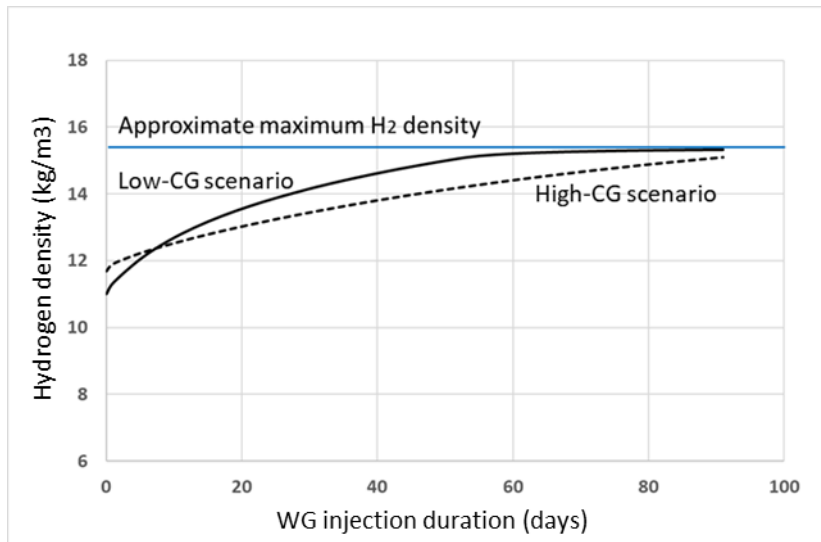

Figure 3: Density change of hydrogen near the injection well during 91 days of WG injection. The blue line highlights the approximate maximum hydrogen density, and hence the maximum hydrogen compression, for this particular cell and scenario. In the high-CG scenario, hydrogen compression is the dominant process and little brine displacement is expected during this period; in the low-CG scenario the brine displacement is much more prominent and hence the pressure and hydrogen density increases much quicker. After 53 days of injection, the pressure has reached the maximum allowed BHP and the injection rate drops. No further compression is possible after this point.

Three months after the WG injection has ceased, the production cycle commences (Figure 2). The WHP and the pressure gradient between the reservoir and the wellhead decreases. However, the 5 MPa WHP constraint is not reached and hence the production rate does not have to be reduced. The example in Figure 2 shows a scenario where the targeted volume of WG cannot be injected and therefore is regarded as an unsuccessful scenario.

Base case scenario

Figure 4 shows the performance of different base case simulation runs with varying CG injection duration. Three components are presented. The first component (dashed black line) shows the mass of injected hydrogen WG relative to the mass of CG in the reservoir. With a CG/WG ratio of less than ~1.27, the targeted mass of hydrogen (1.625 TWh) cannot be achieved within the three-month window; comparable with the scenario in Figure 2 where the injection rate also had to be reduced. With a CG/WG ratio higher than ~1.27, all of the targeted 1.625 TWh of hydrogen can be injected. The CG/WG ratio is calculated based on the actually injected gas, hence although the mass of injected CG decreases by definition to the left, the ratio is kept relatively high because the mass of injected WG also decreases below a CG/WG ratio of ~1.27.
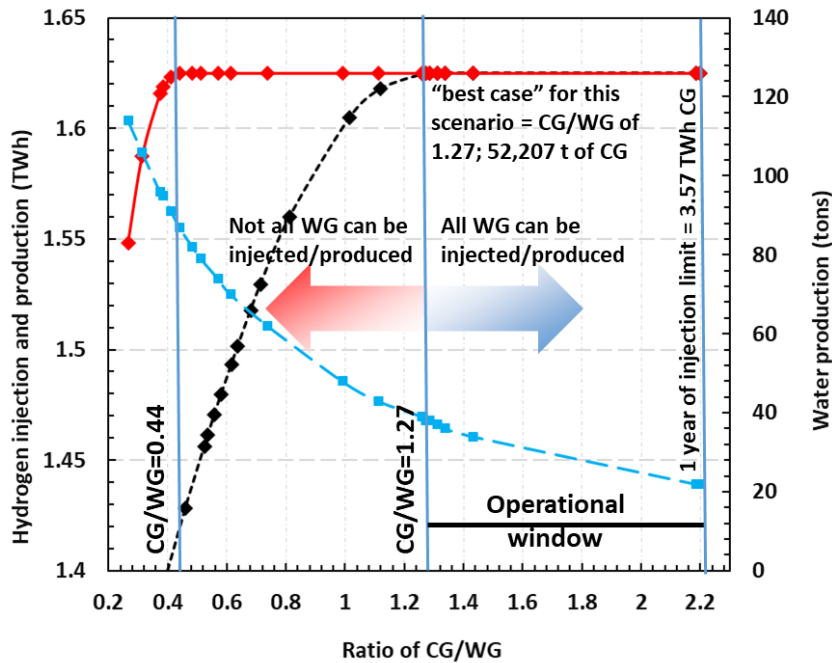
Figure 4: Base case results showing the injection and production performance. The dashed black line represents the amount of hydrogen (in TWh) that can be injected, depending on the CG in place. The red line represents the amount of produced hydrogen (in TWh) that can be produced depending on the CG in place. The targeted total injection and production is 1.625 TWh and this amount of hydrogen can be injected and produced with a CG/WG ratio of 1.27. The blue line shows the amount of water **produced.** *Diamonds represent individual simulation runs.*

The second component of the graph (red line) displays how much CG is required to produce the 1.625 TWh of hydrogen WG. This value needed modification because to the left of the CG/WG ratio of ~1.27, more WG hydrogen is produced than injected. Hence, the mass of CG had to be recalculated by adding the injected CG and WG and subtracting the produced WG. The targeted mass of hydrogen can be produced with a CG/WG ratio of at least 0.44. The graph is limited to the right by the maximum CG/WG ratio which is defined by maximum duration of hydrogen injection of 1 year, during which 3.57 TWh of CG can be injected corresponding maximum CG/WG ratio is 2.20. The "best case" scenario, the scenario with the lowest CG/WG ratio that enables the injection and the production of the 1.625 TWh of hydrogen WG is 1.27. Therefore, the best case and maximum CG/WG ratios range between 1.27 and 2.20 and this is called the "operational window" because within this window the scenario demands are fulfilled.

The third component of the graph in Figure 4 (blue line) shows the produced water during the production process. For the "best case", approximately 38 tons of water are co-produced alongside the hydrogen. The production-limit case with a CG/WG of 0.44 shows a total water production of 87 tons, more than twice the mass.

Sensitivity tests

Figure 5 and Table 3 show the results of the sensitivity tests. Scenarios that failed to inject or produce the targeted 1.625 TWh of hydrogen were due to the BHP reaching the maximum allowed pressure during injection and/or the WHP being too low during production, if not otherwise highlighted in the text. If no data point is displayed, the targeted volume of hydrogen could not be injected or produced regardless of the amount of CG injected.
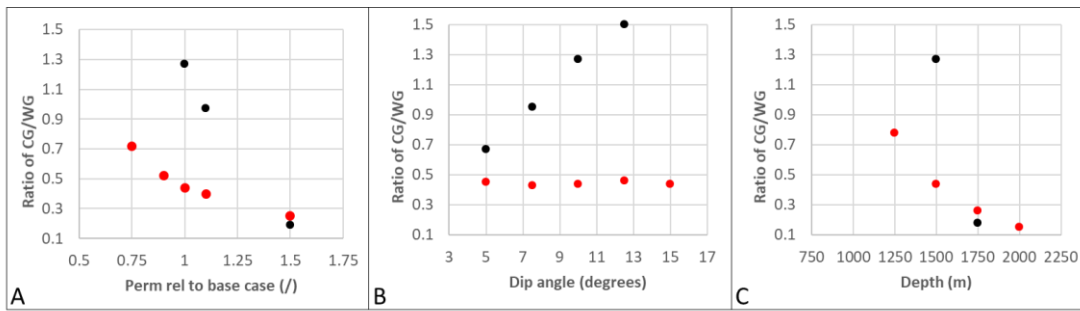
Figure 5: This figure shows the results of the three sensitivity tests, investigating the impact of varying permeability (A), varying anticline dip angle (B) and varying depth (C). The black circles show the "best case" injection performance and the red circles show the "best case" production performance. Absence of circle means that the scenario failed to inject or produce the targeted amount of hydrogen. Note that a "permeability relative to the base case" of 1, a "dip angle" of 10° and a "depth" of 1500 m is the base case, as shown in figure 4.

The sensitivity tests indicate that a higher permeability leads to a lower required CG/WG ratio to inject and produce the targeted amount of hydrogen WG (Figure 5A). No "best case" could be achieved with a permeability of 0.9 and 0.75 times the base case permeability. With a high reservoir permeability of 1.5 times the base case permeability (300 mD / 75 mD for the horizontal and vertical permeability, respectively), a CG/WG ratio of 0.25 is required to inject and produce the targeted volume of hydrogen. The injection process (0.19) requires a lower CG/WG ratio than the production process (0.25). The amount of injected CG over a certain time-period increases with increasing permeability of the storage site. The higher the reservoir permeability, the lower the required CG/WG ratio to produce the targeted 1.625 TWh of hydrogen. The CG/WG ratio required for production ranges from 0.72 for the low permeability scenario to 0.25 for the high permeability scenario.

Table 3: Results of the base case and the sensitivity tests.

Scenario	Maximum CG		Optimal injection	Optimal production	Production constraint	Best case	Water production (Best case)	Limited by
						(CG / WG)		
	(TWh)	(tons)	(CG / WG)	(CG / WG)		WG)	(tons)	
Base case	3.57	90,678	1.27	0.44	WHP	1.27	37	Injection
Permeability sensitivity tests (horizontal / vertical permeability)								
300/75 mD	4.08	103,581	0.19	0.25	WHP	0.25	39	Production
220/55 mD	4.03	102,368	0.97	0.40	WHP	0.97	40	Injection
180/45 mD	3.17	80,487	failed	0.52	WHP	failed	failed	Injection
150/37.5 mD	2.58	65,546	failed	0.72	WHP	failed	failed	Injection

Anticline structure								
5°	3.26	82,687	0.67	0.45	Water	0.67	85	Injection
7.5°	3.67	93,211	0.95	0.43	WHP	0.95	62	Injection
12.5°	3.53	89,570	1.50	0.46	WHP	1.50	32	Injection
15°	3.43	87,016	failed	0.44	WHP	failed	failed	Injection
Storage site depth								
1000 m	1.19	30,182	failed	failed	failed	failed	failed	Injection / Production
1250 m	2.18	55,408	failed	0.78	WHP	failed	failed	Injection
1750 m	4.07	103,343	0.18	0.26	WHP	0.26	93	Production
2000 m	3.26	82,700	<0.03	0.15	WHP	0.15	86	Production

Increasing the dip angle of the anticline limbs results in a "tighter" geological trap structure. Figure 5B shows that a tighter anticline requires a higher CG/WG ratio to inject the 1.625 TWh of hydrogen. For example, a limb angle of 12.5° requires a CG/WG ratio of 1.50 to inject the targeted 1.625 TWh. No "best case" could be achieved with a limb angle of 15°. The lowest required CG/WG ratio of 0.67 was modelled for the 5° dip angle scenario. The production process requires a lower CG/WG ratio compared to the injection process in all the investigated anticline structures. The amount of injected CG over a certain time period increases with the openness (lower dip angle) of the anticline, with a maximum of 3.8 TWh after one year of injection for the 5° anticline, compared to 3.43 TWh for the 15° scenario. The impact of the openness of the anticline on the production performance CG/WG ratio is relatively small, ranging between 0.4 and 0.5, and obvious trends are visible. The production limitation of the 5° scenario is due to the gas-water contact reaching the cell underneath the perforation. The other production scenarios are limited by sub-optimal pressure support.

Figure 5C shows CG/WG ratio scenarios with varying depth in the subsurface. In both scenarios shallower than the base case storage site (1500 m), at top depth of 1250 m and 1000 m, the targeted 1.625 TWh of hydrogen WG could not be injected and hence no "best case" could be achieved, even with the maximum amount of cushion gas. The targeted hydrogen WG could be injected into deeper structures with a very small CG requirement. For example, in the 1750 and 2000 m deep scenarios the injection process requires a lower CG/WG ratio than the production process. The amount of injected CG over a certain time period increases with the depth of the storage site, with 1.19 TWh and 2.18 TWh for the 1000 m and 1250 m deep sites, respectively, compared to 3.57 TWh the 1500 m deep base case. The most efficient CG injection was modelled as 3.26 TWh for the 2000 m deep scenario with 164 days of CG injection. The positive impact of storage depth on the WG production performance is also significant but not as high as the WG injection. Production from the 2000 m deep structures require a CG/WG ratio of 0.15. Under the study conditions, the targeted 1.625 TWh of hydrogen cannot be produced within 91 days from a 1000 m deep structure.
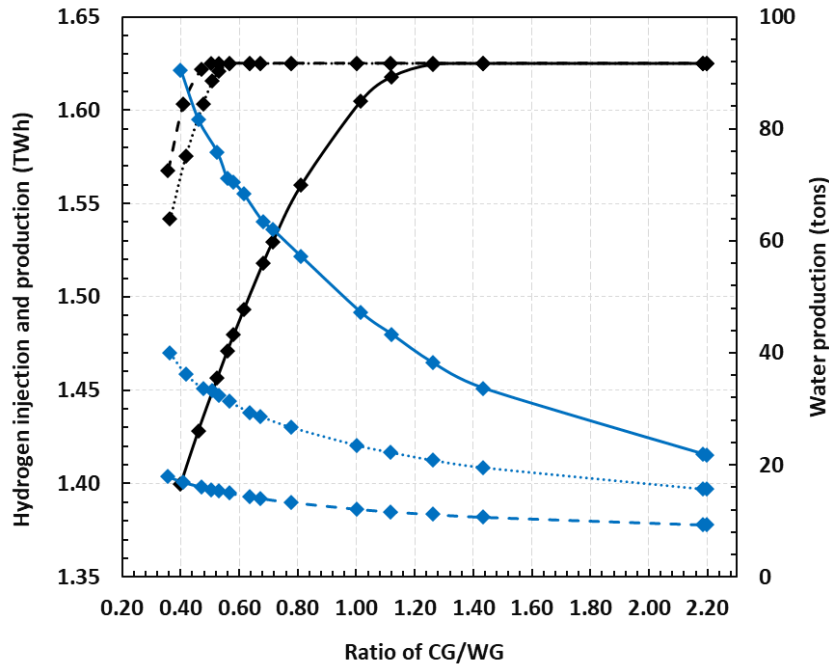
Figure 6: The base case simulation with the WG injection and production repeated in three cycles. Only best-case results are shown, which is the injection performance for all cases. Injection performance is presented in black and water production in blue. The bold line represents the first cycle, with the dotted and dashed lines representing the second and the third cycle, respectively. The figure shows that with every cycle, the storage operation requires less cushion gas and the water production decreases. Diamonds represent individual simulation runs.

When repeating the WG injection and production, the trend towards a WG cycle that requires less cushion gas and that produces less water is visible (Figure 6). At the same time, the pressure in the system decreases slightly as well as the water saturation in the CG saturated zone. The simulation results show a "best case" CG/WG ratio of ~0.6 and ~0.5 for the second and the third cycle, with a much lower water production of 31 and 16 tons, respectively.

Discussion

This study shows that CG is an important component for exploiting the total capacity of a hydrogen storage site. Capacity estimations for gas fields are often based on initial gas in place but this gas has been produced over decades. However, for gas storage the production window is only a few months and hence the production performance has to be high. The results show that for the modelled scenarios, it is possible to inject and reproduce 1.625 TWh (the targeted amount of hydrogen to support one quarter of East Anglia's energy needs), corresponding to 41,244 tons, of hydrogen in an open saline aquifer using one well over a period of three months. The limiting factor for most of the simulations, apart from deeper structures and a very high reservoir permeability, is the injection of the working gas. As hydrogen has a low density, large volumes have to be injected which results in a rapid increase in pressure. The production process is generally very efficient because hydrogen is very mobile and the drawdown pressures are high.

All absolute results in this study have a degree of uncertainty because pressure systems in open, undrilled saline aquifers are usually not well understood and hence their pressure dissipation is uncertain. Modelling studies on hydrogen injection and reproduction (Lubon & Tarkowsky, 2020; Pfeiffer et al. 2017), as well as studies on CO_2 storage (Williams et al., 2013; Ghanbari et al., 2020) have used pore volume modifiers around the reservoir model to simulate an open aquifer. When applied to this study, this method resulted in a more efficient pressure dissipation compared with the Fetkovich analytical aquifer. Test simulations on semi-open systems using the Fetkovich aquifer and an extended numerical aquifer produced promisingly similar results, and therefore the Fetkovich method was chosen over the pore volume multiplier method. Whatever the chosen aquifer simulation methodology, the vital importance of pressure dissipation on the results always introduces a degree of uncertainty without properly history-matched systems. Although this is an uncertainty which impacts the absolute results of the simulations, it will have a lower effect on the relative results and overall trends highlighted by this study.

Another important uncertainty is the limited knowledge of hydrogen fluid flow parameters such as relative permeability, capillary entry pressure and other flow aspects. In order to highlight one example in more detail, there is no data for hysteresis available for a hydrogen – brine system. Gas hysteresis, which defines the residual gas saturation after the water re-migrates into a cell with a certain gas saturation, is an important parameter in CO_2 storage, when the gas plume is expected to migrate over certain distances (Krevor et al., 2015). Migration is not wanted in hydrogen storage but hysteresis may play a role when the displacement of brine is the main process during the injection and production of the WG. If the WG production leads to a rise of the gas water contact, a certain proportion of the hydrogen will be trapped as residual gas. This residual gas should be subtracted from the gas cap as it will not support the production, it will not protect the production well from water influx and it will not assist the next injection cycle by adding to the gas compression process. Experimental studies on hysteresis will help to better asses if, or how much, this effect could increase the CG requirement in aquifer storage.

Storage processes: Gas compression vs brine displacement

The two main storage processes observed in this study are gas compression and decompression, and brine displacement. Even in the simulations with high CG/WG ratios, when gas compression

dominates, the hydrogen plume will grow after the WG injection has stopped and the density of the gas decreases. The basic difference between gas compression and aquifer displacement is the rapid pressure increase during the aquifer displacement dominated injection process, which quickly leads to a decrease of the injection rate. The base case results show that although the pre-injection pressure of a simulation with small volumes of CG is lower, the brine displacement leads to a rapid pressure increase and as a consequence, to a decline of the injection rate. During production, the main driver is the drawdown, the difference of the reservoir pressure and the pressure in the production well. Hence, the production rate is an emptying process that is most effective when the gas pressure in the reservoir is high, either because the reservoir pressure did not equilibrate after injection or because of buoyancy pressure due to a long hydrogen gas leg. This study takes the surface delivery pressure range of 5 MPa into account as the requirements for natural gas transmission in the UK (Dodds et al. 2013). If open well conditions were assumed, the production cycle would be even more efficient.

Permeability, trap structure and depth

A reduction of the permeability has a significant negative effect on the injection because the pressure cannot dissipate efficiently, leading to the maximum allowed BHP being reached very early and hence the injection process being curtailed. High permeability leads to better gas production because the flow rate within the reservoir is increased, fluids can flow to the well more efficiently and therefore the risk of low-pressure zones around the production well, which could result in a reduction of the production rate, is reduced.
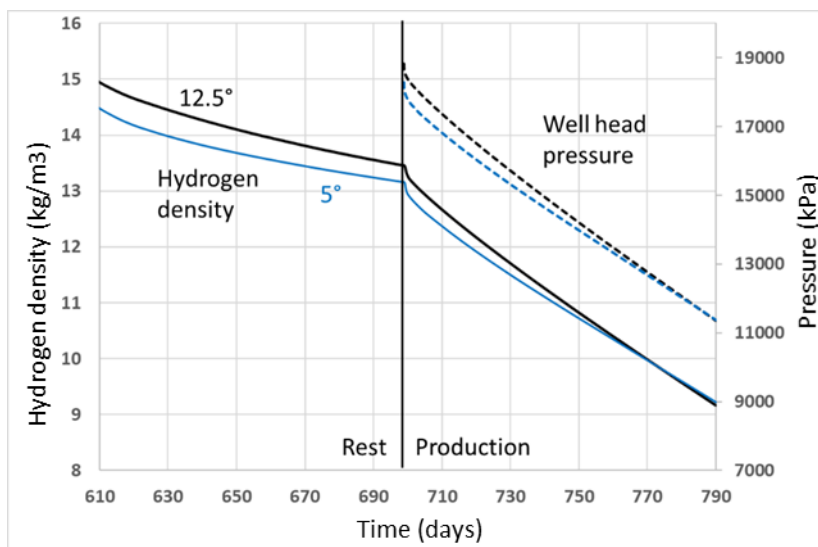

Figure 7: The hydrogen density (solid line) close to the injection well and the WHP (dashed line) of an open (5°) and a tighter (12.5°) anticline before and during production. The data show that after the WG injection, the hydrogen density is higher in the tighter anticline model but the difference is reduced with time. Once production starts, hydrogen density and WHP decrease due to a decrease in pressure, and this decrease is more rapid in the tighter model due to a less efficient pressure equilibration.

In the modelled scenario, tighter anticline structures with higher limb angles reduce the injection performance. Tighter anticlines have smaller gas – water contact areas compared to more open folds, and hence more vertical water displacement is necessary and the hydrogen being transferred

into the deeper part of the model quicker. This results in higher pressures compared to the injection along almost parallel high permeability reservoir layers. The production is not affected by the shape of the anticline and it is suggested here that two processes cancel each other out. It is generally expected that tight anticlines with long gas legs stabilise the production process due to high buoyancy pressures and effective vertical migration towards the production well, and additionally it was suggested in the literature that tight anticlines prevent hydrogen from spreading out and becoming unrecoverable (Panfilov, 2010; Hagemann et al., 2015). However, the present study cannot provide conclusive evidence for or against this statement, mainly because the grid size is too large and it would probably require a more realistic irregular shape and reservoir heterogeneity to analyse this. As hydrogen has a low density and therefore large volumes have to be produced to reach the 1.625 TWh target, the rapid production requires the gas-water contact to rise quickly in order to equilibrate production induced low pressure in the gas cap. In a tight anticline trap structure, this does not happen and a low-pressure zone in the gas cap develops which ultimately reduces the hydrogen production. These two effects seem to be in balance in this scenario. As this inability of the gas-water contact to rise quickly is regarded as a problem here because it limits the productivity, it should be added that this gas expansion of the gas cap also limits aquifer influx.

A deeper structure is generally favourable for both hydrogen injection and production. A major impact on injection is the calculated fracture gradient. The BHP fluctuates roughly between the hydrostatic pressure and the maximum allowed pressure. This maximum pressure is defined as 90 % of the fracture pressure, which in itself is calculated with the lithostatic pressure. By definition, the hydrostatic pressure increases with depth with a slower rate than the fracture pressure. The pressure between hydrostatic pressure and the maximum allowed BHP increases with depth. As a consequence, there is a trend in the pressure window whereby the deeper the site, the more pressure increase is sustainable and the higher the possible injection rates. It should be mentioned here that a different interpretation of reservoir safety, for example a less conservative definition of the maximum allowed BHP, will lead to different injection performances. The production benefits from the generally higher pressure in deeper reservoirs, which leads to an increase of the drawdown pressure between the reservoir and the wellhead, and from the smaller, denser hydrogen cap around the production well.

Multiple storage cycles

If the WG cycle is repeated, the injection process requires less CG to inject the WG due to a decrease in pressure within the reservoir system. This pressure decrease is highest between cycle one and two, and significantly smaller between cycle two and three. As the same amount of WG is extracted and re-injected during the cycles, the amount of gas in the system does not change significantly. However, other factors can change the reservoir pressure: Firstly, the pressure increase during CG injection. The actual pressure increase is not higher compared with the WG injection stage, but the CG related pressure increase is not eliminated by a WG production cycle. Hence, the first WG injection will occur in an already pressurised system. A possible strategy to mitigate this effect would be to increase the rest stage between the CG and WG injection. Secondly, pore water is extracted during every production cycle, especially during the first. However, this contribution is assumed to be small because the water volume extracted is rather small compared to the overall aquifer size. Both processes will reduce their impact with increasing cycle numbers, as seen in Figure 6, and a

stabilisation of the system is expected. The simulation results show that if the first cycle is successful, subsequent cycles are likely to be successful too.

Water production is problematic because water has to be extracted from the produced gas, and it poses the risk of water accumulating in the production tubing, also referred to as liquid loading (Lea et al., 2008; Riza et al., 2016). In this study, liquid loading is partially controlled by monitoring the gas-water contact in order to keep high levels of flowing water away. If the production perforation were to submerge, the gas pressure behind the perforation would have to overcome the pressure of an extensive water column in the well, which would result in a drop in productivity. Although this problematic for the production of gas fields, it might not be a major risk in a gas storage operation, where the accumulated water could be flushed out during the next injection cycle. However, it is under no circumstances a desirable scenario and will always interrupt the storage operation. Generally, water production increases with a decreasing CG/WG ratio. For example, the more CG is in place, the more effectively the water is kept at a safe distance from the injection well. Water production is high for best case production scenarios with low reservoir permeability and open anticline structures. Water production decreases significantly with increasing cycle numbers, because with every cycle the amount of mobile water in the hydrogen cap is further decreased, until almost depleted gas field conditions are reached, and the hydrogen gas phase can flow more efficiently.

Next steps

There are several geological and technical parameters, which have not been investigated in this study. Well specifications such as the well diameter or the perforation length will certainly have an impact, but as this study has shown that pressure dissipation is dominating the injection and the production process, the well specifications will have a more nuanced impact. Geological variations such as the reservoir thickness will also be of importance, with an increasing reservoir thickness leading to a more efficient pressure dissipation. Another aspect that has not been considered in this study is reservoir heterogeneity, which will determine the injection and production performance in the reservoir. Heterogeneity in reservoirs refers to mm- to m-scale variability in the composition of the rock (e.g. grain size, sorting, lamination) and architectural variability associated with depositional processes (e.g. cross-stratification and channelisation) often leading to reservoirs being interlaced by non-reservoir rock. Complex lithofacies can have a high impact on the flow paths for the stored gas as well as on the pressure dissipation and hence their characterisation is of vital importance for the accurate simulation of hydrogen storage scenarios (Williams et al., 2013; Lengler et al., 2010). In heterogeneous reservoirs, most of the injected gas flow as well as the pressure flow will occur in the high-permeability channels and layers, and hence the reliable prediction of how fast and how far the highly mobile hydrogen flows, will require a detailed understanding of the high-permeability reservoir zones. Depleted gas fields have a wealth of data leading to a better understanding of the geological heterogeneities than potential hydrogen storage sites in saline aquifers. The initially limited understanding of the reservoir geology has to be improved in order to confirm the storage capacity estimates and minimise the uncertainty in locating the high-permeability zones to guarantee that injection and production wells operate with maximum effectiveness. If a targeted reservoir is missed or has poorer reservoir properties than previously anticipated, injectivity and productivity could be greatly reduced. Most of this is well known and proven in hydrocarbon fields

with a long production history, which is an important advantage of hydrogen storage in depleted gas fields compared to saline aquifer storage.

CG is an upfront cost for any gas storage operation. However, this study shows that although large volumes of CG are not always required, it has a net positive effect on the storage operation. Most significantly, CG in place reduces the need for brine displacement during the WG injection, which makes the WG injection less energy intense, increases the injection performance in most cases and reduces the volume of co-produced water. Future work should, using real-world storage sites, focus on the economic benefit of the one-time CG injection on the WG injection and production cycles compared with the cost of the injected CG. This is relevant for storage operations in saline aquifers as well as depleted gas fields with aquifer support.

Conclusion

Hydrogen storage in open saline aquifers is a promising alternative to hydrogen storage in depleted gas fields, but detailed site characterisation as well as an investigation into the pressure equilibration capability is important as pressure dissipation is the main geological process determining the injectivity and productivity of hydrogen in a saline aquifer.

Cushion Gas is one of the main factors controlling both injectivity and productivity of hydrogen, and hence has a direct impact on storage capacity. CG cannot increase the total storage capacity of a storage site, but it is an important component for exploiting the available storage capacity as efficiently as possible.

The CG/WG ratio required varies significantly (for the first injection cycle between 0.15 and 1.5 in this study) depending on the three geological parameters investigated in this study (reservoir depth, the shape of the trap, and reservoir permeability). Additionally, the targeted WG volume will also have a major control on the amount of CG needed. This shows that rule-of-thumb CG estimations are often mere guesswork and numbers should be refined early on in projects in order to achieve more reliable cost estimates. Future work should investigate the cost benefit of CG for WG injection and production vs the one-time CG investment.

Hydrogen storage in deeper structures and reservoirs with higher reservoir permeabilities requires a lower CG/WG ratio. Storage in tight anticlines makes injection more difficult and has little impact on the production, for the analysed scenarios. However, water production increases with more open structures. With subsequent cycles, the required CG/WG ratio and the volume of produced water decreases, and if the first cycle is successful, subsequent cycles are likely to be successful too.

Acknowledgment

References

Alcalde, J., Flude, S., Wilkinson, M., Johnson, G., Edlmann, K., Bond, C.E., Scott, V., Gilfillan, S.M.V., Ogaya, Xenia, Haszeldine, R.S., 2019. Estimating geological CO2 storage security to deliver on climate mitigation. Nature Communications, 9, 2201. https://doi.org/10.1038/s41467-018-04423-1

Alcalde J, Heinemann N, Mabon L, Worden RH, de Coninck H, Robertson H, Maver, M., Ghanbari, S., Swennenhuis, F., Mann, I., Walker, T., Gomersal, S., Bond, C.E., Allen, M.J., Haszeldine, R.S., James, A., Mackay, E., Brownort, P.A., Faulkner, D.R., Murphy, S., 2019. Developing full-chain industrial carbon capture and storage in a resource- and infrastructure-rich hydrocarbon province. Journal of Cleaner Production, 233. https://doi.org/10.1016/j.jclepro.2019.06.087.

Amid, A., Mignard, D., Wilkinson, M., 2016. Seasonal storage of hydrogen in a depleted natural gas reservoir. International Journal of Hydrogen Storage, 41. http://dx.doi.org/10.1016/j.ijhydene.2016.02.036

Aziz, K., Govier, G.W., 1972. Pressure drop in wells producing oil and gas. Journal of Canadian Petroleum Technology, 11/3. doi: 10.2118/72-03-04.

Basso, O., Lascourreges, J.F., Le Borgne, F., Le Goff, C., Magot, M., 2009. Characterization by culture and molecular analysis of the microbial diversity of a deep subsurface gas storage aquifer. Research in Microbiology, 160. DOI: 10.1016/j.resmic.2008.10.010

Bentham, M., 2006. An assessment of carbon sequestration potential in the UK – Southern North Sea case study. Tyndall Centre for Climate Change Research, Working Paper 85.

Carden, P.O., Paterson, L., 1979. Physical, chemical and energy aspects of underground hydrogen storageInt. International Journal of Hydrogen Energy, 4, 559–569. https://doi.org/10.1016/0360-3199(79)90083-1

CMG, 2019. 'GEM'. Available at: https://www.cmgl.ca/gem.

Dodds, P.E., Demoullin, S., 2013. Conversion of the UK gas system to transport hydrogen. International Journal of Hydrogen Energy, 38/18. https://doi.org/10.1016/j.ijhydene.2013.03.070

Engeland, K., Borga, M., Creutin,, J.D., Francois, B., Ramos, M.H., Vidal, J.P., 2017. Space-time variability of climate variables and intermittent renewable electricity production – A review. Renewable Sustainable Energy Reviews, 79, 600–617. https://doi.org/10.1016/j.rser.2017.05.046

European Commission, 2015. The role of gas storage in internal market and in ensuring security of supply. https://ec.europa.eu/energy/sites/default/files/documents/REPORT-Gas%20Storage-20150728.pdf

Feldmann, F., Hagemann, B., Ganzer, L., Panfiloc, M., 2016. Numerical simulation of hydrodynamic and gas mixing processes in underground hydrogen storages. Environmental Earth Science, 75. https://doi.org/10.1007/s12665-016-5948-z

Fetkovitch, M.J., 1971. A simplified approach to water influx calculations – Finite aquifer systems. Journal of Petroleum Technology, 23, 814-828. https://doi.org/10.2118/2603-PA

Gammer, D., Green, A., Holloway, S., Smith, G., 2011. The Energy Technologies Institute's UK CO2 Storage Appraisal Project (UKSAP). In: SPE 148426, Presented at the SPE Offshore Europe Oil and Gas Conference and Exhibition, Aberdeen, UK. 6–8 September 2011.

Ghanbari, S., Mackay, E.J., Heinemann, N., Alcalde, J., James, A., Allen, M., 2020. Impact of CO2 mixing with trapped hydrocarbons on CO2 storage capacity and security: A case study from the Captain Aquifer (North Sea). Applied Energy, 278. https://doi.org/10.1016/j.apenergy.2020.115634

Gluyas, J.G., Hichens, H.M., 2003. The United Kingdom oil and gas fields commemorative millennium volume. Gluyas, J.G., Hichens, H.M. (edts): Memoirs of the Geological Society of London.

Gregory, S.P., Barnett, M.J., Field, L.P., Milodowski, A.E., 2019. Subsurface microbial hydrogen cycling: Natural occurrence and implications for industry. Microorganisms, 7, 53.

Hagemann, B., Rasoulzadeh, M., Panfilov, M., Ganzer, L., Reitenbach, V., 2015. Mathematial modelling of unstable transport in underground hydrogen storage. Environmental Earth Science, 73, 6891-6898. DOI 10.1007/s12665-015-4414-7

Heinemann, N., Alcalde, J., Miocic, J.M., Hangx, S.J.T., Kallmeyer, J., Ostertag-Henning, C., Hassanpouryouzband, A., Thaysen, E.M., Strobel, G.J., Schmidt-Hattenberger, C., Edlmann, K., Wilkinson, M., Bentham, M., Haszeldine,R.S., Carbonell, R., Rudloff, A., 2021. Enabling large-scale hydrogen storage in porous media – the scientific challenges. Energy and Environmental Science, 14, 853-864. https://doi.org/10.1039/D0EE03536J

Heinemann, N., Booth, M.G., Haszeldine, R.S., Wilkinson, M., Scafidi, J., Edlmann, K., 2018. Hydrogen storage in porous geological formations – Onshore play opportunities in the Midland Valley (Scotland, UK). International Journal of Hydrogen Energy, 43/45, 20861-20874. https://doi.org/10.1016/j.ijhydene.2018.09.149

IPCC, 2018: Global Warming of 1.5°C.An IPCC Special Report on the impacts of global warming of 1.5°C above pre-industrial levels and related global greenhouse gas emission pathways, in the context of strengthening the global response to the threat of climate change, sustainable development, and efforts to eradicate poverty (Masson-Delmotte, V., P. Zhai, H.-O. Pörtner, D. Roberts, J. Skea, P.R. Shukla, A. Pirani, W. Moufouma-Okia, C. Péan, R. Pidcock, S. Connors, J.B.R. Matthews, Y. Chen, X. Zhou, M.I. Gomis, E. Lonnoy, T. Maycock, M. Tignor, and T. Waterfield (eds.)).

Jossi, J.A., Stiel, L.I., Thodos, G., 1962. The viscosity of pure substances in the dense gaseous and liquid phases. American Institute of Chemical Engineers Journal, 8/1, 59-63. https://doi.org/10.1002/aic.690080116

Krevor, S., Blunt, M.J., Benson, S.M., Pentland, C.H., Reynolds, C., Al-Menhali, A., Niu, B., 2015. Capillary trapping for geologic carbon dioxide storage – From pore scale physics to field scale implications. International Journal of Greenhouse Gas Control, 40. https://doi.org/10.1016/j.ijggc.2015.04.006

Kunz, O. & Wagner, W., 2012. The GERG-2008 Wide-Range Equation of State for Natural Gases and Other Mixtures: An Expansion of GERG-2004. Journal of Chemical Engineering Data, 12/57, 11, 3032-3091. https://doi.org/10.1021/je300655b

Le Fevre, C., 2013. Gas storage in Great Britain. https://www.oxfordenergy.org/wpcms/wp-content/uploads/2013/01/NG-72.pdf.

Lea, J.F., Nickens, H.V., Wells, M.R., 2008. Gas well deliquification. Gulf, Drilling Guides, Gulf Professional Publishing. https://doi.org/10.1016/B978-0-7506-8280-0.X5001-X

Leachman, J.W., Jacobsen, R.T., Penoncello, S.G. & Lemmon, E.W., 2009. Fundamental equation of state for parahydrogen, normal hydrogen and orthohydrogen. Journal of Physical and Chemical Reference Data, 38. https://doi.org/10.1063/1.3160306

Lengler, U., De Lucia, M., Kuehn, M., 2010. The impact of heterogenity on the distribution of CO_2: Numerical simulation of CO_2 storage in Ketzin. International Journal of Greenhouse Gas Control, 4/6. https://doi.org/10.1016/j.ijggc.2010.07.004

Lohrenz, J., Bray, B.G., Clark, C.R., 1964. Calculating Viscosities of Reservoir Fluids from their compositions. Journal of Petroleum Technology, SPE Paper 9151171-1176. https://doi.org/10.2118/915-PA

Lubon, K., Tarkowski, R., 2020. Numerical simulation of hydrogen injection and withdrawal to and from a deep aquifer in NW Poland. International Journal of Hydrogen Energy, 45, 2068 – 2083, https://doi.org/10.1016/j.ijhydene.2019.11.055

Matos, C.R., Carneiro, J.F., Silva, P.P., 2019. Overview of Large-Scale Underground Energy Storage Technologies for Integration of Renewable Energies and Criteria for Reservoir Identification. Journal of Energy Storage, 21, 241-258. https://doi.org/10.1016/j.est.2018.11.023

Mouli-Castillo, J., Heinemann, N., Edlmann, K., 2021. Mapping geological hydrogen storage capacity and regional heating demands: An applied UK case study. Applied Energy, 283, 116348. https://doi.org/10.1016/j.apenergy.2020.116348

Oil and gas field data from the North Sea [Internet]. Oil and Gas Authority 2020 [cited 19.5.2020]. Available from: https://www.ogauthority.co.uk/data-centre/.

Panfilov, M., 2010. Underground Storage of Hydrogen: In Situ Self-Organisation and Methane Generation. Transport in Porous Media, 85, 841–865, https:// doi.org/10.1007/s11242-010-9595-7

Panfilov, M., 2016. Underground and pipeline hydrogen storage, 91–115. In: R.B. Gupta, A. Basile, T. Nejat Veziroglu (edts): Compendium of Hydrogen Energy, Volume 2: Hydrogen Storage, Distribution and Infrastructure.

Paterson, L., 1983. The implications of fingering in underground hydrogen storage. International Journal of Hydrogen Energy, 8/1, 53–59. https://doi.org/10.1016/0360-3199(83)90035-6

Peaceman, D.W., 1983. Interpretation of well-block pressures in numerical reservoir simulation with nonsquare grid blocks and anisotropic permeability. SPE Journal, 23.

Peaceman, D.W., 1987. Interpretation of well-block pressures in numerical reservoir simulation: Part 3: Off-center and multiple wells within a well-block. SPE 16976, SPE Annual Technical Conference and Exhibition, Dallas, TX, September 27-30.

Pfeiffer, W.T., Beyer, C., Bauer, S. 2017. Hydrogen storage in a heterogeneous sandstone formation: dimensioning and induced hydraulic effects. Petroleum Geoscience, 23, 315–326. https://doi.org/10.1144/petgeo2016-050

Riza, M.F., Hasan, A.R., Kabir, C.S., 2016. A pragmatic approach to understanding liquid loading in gas wells. SPE Production & Operations, 31/03, 185–196, SPE-170583-PA. https://doi.org/10.2118/170583-PA

Scafidi, J., Wilkinson, M., Gilfillan, S.M.V., Heinemann, N., Haszeldine, R.S., 2021. A quantitative assessment of the hydrogen storage capacity of the UK continental shelf. International Journal of Hydrogen Energy, 46/12. https://doi.org/10.1016/j.ijhydene.2020.12.106

Stiel, L.I., Thodos, G., 1961. The viscosity of nonpolar gases at normal pressures. American Institute of Chemical Engineers Journal, 7/4, 611-615. https://doi.org/10.1002/aic.690070416

Tarkowski, R., 2019. Underground hydrogen storage: Characteristics and prospects. Renewable & Sustainable Energy Reviews, 105, 86-94. https://doi.org/10.1016/j.rser.2019.01.051

Thaysen, E.M., McMahon, S., Strobel, G.J., Butler, I.B., Ngwenya, B.T., Heinemann, N., Wilkinson, M., Hassanpouryouzband, A., McDermott, C., Edlmann, K., 2021. Estimating Microbial Growth and Hydrogen Consumption in Hydrogen Storage in Porous Media. Accepted in Renewable and Sustainable Energy Reviews.

Wallace, R.L., Cai, Z., Zhang, H., Zhang, K., Guo, C., 2021. Utility-scale subsurface hydrogen storage: UK perspectives and technology. International Journal of Hydrogen Energy, 46/49, 25137-25259. https://doi.org/10.1016/j.ijhydene.2021.05.034

Wilhelms, A., Larter, S.R., Head, I., Farrimond, P., di-Primio, R., Zwach, C., 2000. Biodegradation of oil in uplifted basins prevented by deep-burial sterilization. Nature, 411, 1034–1037. https://doi.org/10.1038/35082535

Williams, J.D.O., Jin, M., Bentham, M., Pickup, G.E., Hannis, S.D., Mackay, E.J., 2013. Modelling carbon dioxide storage within closed structures in the UK Bunter Sandstone Formation. International Journal of Greenhouse Gas Control, 18. http://dx.doi.org/10.1016/j.ijggc.2013.06.015

Yekta, A.E., Manceau, J.-C., Gaboreau, S., Pichavant, M., Audigane, P., 2018. Determination of Hydrogen–Water Relative Permeability and Capillary Pressure in Sandstone: Application to Underground Hydrogen Injection in Sedimentary Formations. Transport in Porous Media, 122. https://doi.org/10.1007/s11242-018-1004-7